EUROPEAN CONFERENCE ON INTEGRATED OPTICS

Integrated four channel wavelength multiplexer in Thin Film Lithium Niobate for CWDM 400G/800G short reach communications

Giuseppe Cusmai[1], Riccardo Marchetti[1], Piero Orlandi[1], Andrea Martellosio[1] and Roberto Longone[1]

[1] Advanced Fiber Resourced – San Donato Milanese, 20097 Italy
[*] giuseppe.cusmai@fiber-resources.com

A four-channel multiplexer operating in the O-band for 400GBASE-FR4 and 800G-2xFR4 applications is demonstrated on Thin Film Lithium Niobate. Critical phase error arising from fabrication process is analysed. Design improvements are discussed to increase multiplexer tolerance to phase error.
Keywords: *LNOI, multiplexer, lithium niobate, optical waveguides*

INTRODUCTION

Over the last few years Thin Film Lithium Niobate (TFLN) arose as a very promising technological platform for several applications. The possibility for new generation devices, complex architectures with small footprints and low losses have made TFLN attractive in different fields such as telecommunication and datacom, quantum photonics and sensing. This is due, from one side, to the excellent properties of LiNbO3 (electro-optic, nonlinear-optic, acousto-optic, piezoelectric and pyroelectric) and from the other side to the high integration potential enabled by the high index contrast. Datacom applications are of particular interest since costs, footprint, bandwidth and losses are critical requirements. These requirements can be met only by a technological platform able to integrate various functionality on a single chip as, for example, wavelength management in case of CWDM communication protocols. Key CWDM-based protocols for the development of short reach intra-datacenter communications (from 500 m up to 2 Km) are the 400GBASE-FR4 and the 800G-2xFR4. The first, addressing 400 Gigabit ethernet links through a 4 channels CWDM system, the latter addressing 800 Gigabit ethernet links through a system based on two parallel 4 channels CWDM lanes. Both operating in the O-band. Fundamental building blocks for these applications are wavelength multiplexer (MUXes) and de-multiplexers (DE-MUXes). Different solutions providing wavelength multiplexing have been proposed in many integrated photonics platforms [1-3] but the most performing in terms of insertion loss and crosstalk are based on interferometric filters, enabling very high flat top optical responses [4]. On the other hand, a severe drawback for these architectures is the high sensitivity to interferometric paths phase errors which are linked to technological limits in controlling optical waveguides characteristics (i.e., side-wall roughness, etch depth, film thickness and refractive index uniformity) [3]. On more mature platforms this issue has been reasonably solved [3], while recent TFLN platforms are still struggling to achieve a process control in waveguide definition enabling acceptable phase errors for passive interferometric structures designs.

In this work we present a passive MUX fabricated on 4” TFLN X-Cut wafers for transmitters targeting FR4 and 2xFR4 applications. The architecture is based on well-known cascaded Mach Zehnder Interferometers (MZIs) lattice filters [6]. A statistical analysis of the results obtained on several realizations of the device is presented. Then, through a comparison between statistical experimental data and theory the process phase error has been quantified. Finally, some considerations on possible design improvements to increase tolerance to process fluctuations are presented.

DESIGN AN MODELING

X-Cut TFLN wafers are considered for the design and realization of the device. The simulated waveguide cross section is reported in Fig.1(a).

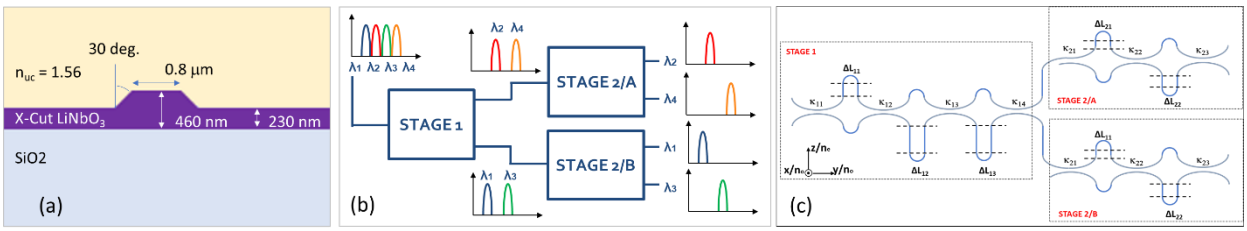

Fig. 1. (a) Waveguide cross section. (b) Block diagram schematics of the multiplexer. (c) Schematics of the multiplexer stages.

A LiNbO3 film thickness of 460 nm and an etch depth of 230 nm has been set to minimize polarization rotation effects that might occur due to TE and TM modes hybridization [7,8]. A 0.8 μm waveguide width ensures single mode operation in the O-band. A waveguide sidewall angle of 30° is then considered as representative of the final waveguide shape due to the etching process. An upper cladding with refractive index n_{uc}=1.56 at 1310 nm is taken into account. Under these conditions the quasi-TE fundamental mode effective index and group index are n_{effY}=1.900, n_{gY}=2.206 along crystal Y-axis propagation direction (Y-prop) and n_{effZ}=1.967, n_{gZ}=2.354 along crystal Z-axis propagation direction (Z-prop).

The proposed 4-channels CWDM MUX is based on a double stage cascaded MZIs lattice filters according to [4,5] and schematically reported in Fig.1(b) and Fig.1(c). Stage1 combines odd and even channels couples with a free spectral range (FSR) equal to 20 nm. Stage2/A and Stage2/B combine respectively even and odd channels with FSR = 40nm. Channels central wavelengths are λ_1=1271 nm, λ_2=1291 nm, λ_3=1311 nm and λ_4=1331 nm. In-band channel spectral response flat top shape is increased as the number of MZIs is increased within each stage. For Stage1 the choice has been to use 3 lattices cascaded MZIs, while only 2 are used in Stage2/A and Stage2/B. Coupling coefficients κ_{ij} and geometrical length imbalance ΔL_{ij} (where i refers to the stage number and j to the device number within the stage) are set to: κ_{11}=0.5, κ_{12}=0.2, κ_{13}=0.2, κ_{14}=0.04, $\Delta L_{11}=\Delta L$, $\Delta L_{12}=2*\Delta L$, $\Delta L_{13}=2*\Delta L+\Delta L_\pi$ for Stage1 and κ_{21}=0.5, κ_{22}=0.29, κ_{23}=0.08, $\Delta L_{21}=\Delta L/2$, $\Delta L_{22}=\Delta L$ for Stage2, where ΔL=36.45 μm and ΔL_π=0.33 μm for Stage1, ΔL=18.5 μm for Stage2/A and ΔL=18.22 μm for Stage2/B. The complete device ends up having a total of 14 interferometric paths (3 in Stage1 = 6 arms, 2 in Stage2/A = 4 arms, 2 in Stage2/B = 4 arms).

To minimize phase error effects due to mode conversion, length imbalances are designed in Z-prop exploiting the higher birefringence between the first quasi-TE and first quasi-TM mode. Bend waveguides with bending radius equal to 100 μm have been used to ensure negligible radiation losses. Given this, the simulated ideal transfer functions are reported in Fig.2(a) as dashed black lines.

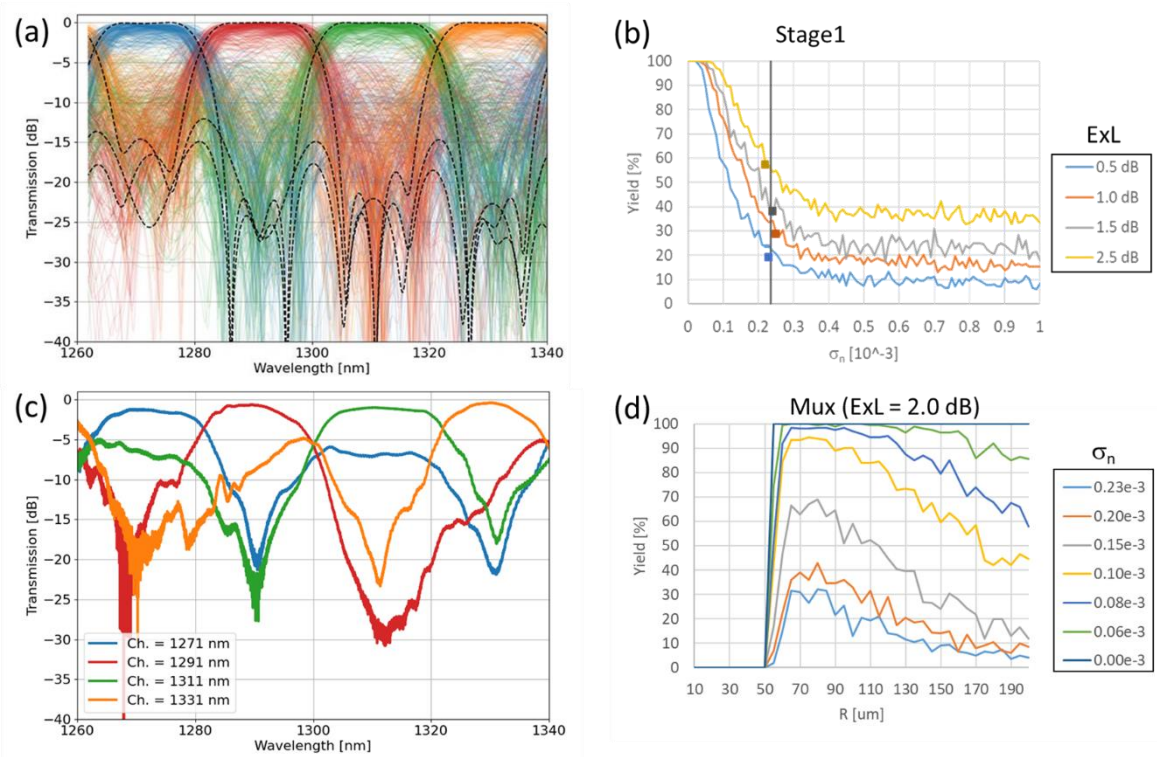

Fig.2. (a) Simulated ideal transfer functions (dashed) of the MUX and effects of random phased errors on the MZIs arms. (b) Stage1 simulated and experimental (squares) yield as a function of σ_n and pass/fail threshold ExL. (c) Measured performance of a fabricated MUX having ExL=2.0 dB. (d) MUX yield as a function of bending radius R and σ_n for ExL = 2.0 dB.

To model the impact of phase error on device performances, we have added a random phase to each optical path of the interferometers $\Delta\phi_v = (2\pi/\lambda)nL_v$ (v=1 to 14) where n is a gaussian stochastic variable with mean equal to 0 and standard deviation equal to σ_n, L_v is the geometrical length of the considered path. In Fig.2(a) as transparent lines are reported the simulated transfer functions obtained in case of 100 realizations with σ_n=0.1e-3. The larger σ_n the greater is the detrimental effect. To quantify the detrimental effect as a function of σ_n we have set the quality parameter as the maximum loss among the channels central wavelengths (MaxLoss) and defined a yield as the ratio between pass and overall realizations where pass are the realizations respecting MaxLoss < ExL being ExL the

threshold value for the pass/fail criteria. Simulated results limited to Stage1 only are reported in Fig.2(b) as solid lines in case of 100 realizations for each value of σ_n and ExL. With the considered conditions, a σ_n <= 0.1e-3 should be attained to provide high yield.

EXPERIMENTAL RESULTS AND ANALYSIS

800G-2xFR4 transmitters have been fabricated using commercially available 4'' LNOI X-Cut wafers. Low-loss waveguides (<0.25 dB/cm), electro-optic modulators, grating couplers (for testing and monitoring Photodiodes), Spot Size Converters (SSC) edge couplers (<1.5 dB/interface) and the 2 multiplexers have been defined with ICP process. To analyze the impact of the phase errors on the MUX, a stand-alone MUX as well as a Stage1-only interleaver structure have been fabricated. An example of a fabricated MUX with ExL=2.0dB is reported in Fig.2(c).

By comparing model predictions and experimental yield of Stage1 fabrications (over 60) as a function of ExL, we have estimated σ_n as reported in Fig.2(b) (square symbols). By setting ExL to 0.5dB, 1.0dB, 1.5dB and 2.5dB we have obtained yields of 19%, 28.6%, 38.1% and 57.1% respectively. The four experimental points match the theoretical curves if σ_n=0.23e-3.

To improve tolerance, we have simulated yield of the MUX as a function of σ_n and a design radius of curvature including radiation and propagation losses in the model. Results are reported in Fig.2(d). Maximum yields are achieved for bending radius equal to 80 μm which turns out to be the best compromise between radiation, propagation losses and device footprint. With σ_n =0.23e-3 a maximum yield of 30% is foreseen. With process improvement enabling σ_n =0.1e-3 a yield above 90% can be reached.

DISCUSSION

Experimental data of the designed multiplexer structures fabricated on a 4" X-Cut TFLN wafers have been analyzed to gather yield statistics based on a variable value of pass/fail criteria (maximum channel insertion loss).

By comparing the experimental and theoretical yield as a function of pass/fail loss threshold, we have determined process phase error standard deviation to be σ_n=0.23e-3.

Our model prediction is that tolerance to process phase errors can be improved by reducing building blocks footprint acting for instance on the choice of maximum bending radius which should be the best tradeoff between radiation, propagation losses and device footprint. Optimum radius of curvature turns out to be 80 μm. Moreover, process improvements decreasing σ_n to 0.1e-3 would enable multiplexer yields up to 90%. Future designs will be aimed to confirm this theoretical prediction.

References

[1] Y. Hu et al., *MMI for wavelength filtering and WDM on the SOI platform*, in Proceedings of IEEE Photonic Society 24th Annual Meeting, pp. 615-616, 2011

[2] W. Shi et al., *Ultra-compact, flat-top demultiplexer using anti-reflection contra-directional couplers for CWDM networks on silicon*, Optics express, vol. 21, no. 6, pp. 6733-6738, 2013

[3] Gengxin Chen et al., *Four-channel CWDM device on a thin-film lithium niobate platform using an angled multimode interferometer structure*, Photonics Research vol. 10, no. 1, pp. 8-13, 2022

[4] S. S. Cheung and M. R. T. Tan, *Silicon nitride (Si_3N_4) (De-)multiplexers for 1-μm CWDM optical interconnects*, Journal of Lightwave Technology, vol. 38, no. 13, pp. 3404-3413, 2020

[5] S. Dwivedi et. al, *Coarse wavelength division multiplexer on silicon-on-insulator for 100 GbE*, in IEEE 12th International Conference on Group IV Photonics (GFP), pp. 9-10, 2015

[6] F. Horst et al., *Cascaded Mach-Zehnder wavelength filters in silicon photonics for low loss and flat pass-band WDM (de-) multiplexing*, Optics express, vol. 21, no. 10, pp. 11652-11658, 2013

[7] C. K. Madsen, J. H. Zhao, *Optical filter design and analysis*, Wiley, New York, 1999.

[8] G. Cavicchioli et al., *Mitigating Polarization Rotation Effects in Thin-Film Lithium Niobate Waveguides*, in Proceedings of 23rd European Conference on Integrated Optics, pp. 45-47, 2022

[9] A. Pan et al., *Fundamental mode hybridization in a thin film lithium niobate ridge waveguide*, Optics Express, vol. 27, no. 24, 2019.